POTHOLE DETECTION AND ROAD CONDITION ASSESSMENT USING HYPERSPECTRAL IMAGERY

Christopher M. Jengo, Senior Consulting Engineer
David Hughes, Senior Consulting Engineer
Research Systems, Inc.
2600 Park Tower Dr., Suite 601, Vienna, VA 22180
cjengo@rsinc.com
dhughes@rsinc.com

Joseph D. LaVeigne*, Staff Scientist
SpecTIR Corporation
1325 Airmotive Way, Suite 375, Reno, NV 89502

Ivan Curtis, Founder
IK Curtis Services, Inc.
2501 West Burbank Blvd., Suite 301
Burbank, CA 91505
ivan@ikcurtis.com

ABSTRACT

The objective of this study is to characterize the quality of road conditions in a semi-automated manner using hyperspectral imagery. High resolution aerial photography collected simultaneously and limited ground photography in the study area serve as surrogate ground truthing used to collect training and validation points. A variety of classification methods are employed. These methods range from those that measure spectral shape to those that measure similarity in brightness, and hybrids that combine the two. In addition, Classification and Regression Tree (CART) algorithms are used. The CART algorithms produce the best results, with classification accuracies of approximately 68%. Classification methods that incorporate brightness are next best (~50% accuracies), while spectral shape based methods perform poorly (~38%). The mediocre results are attributed to the extremely similar spectral characteristics of the mapped materials, all of which are some variation of asphalt. Cracks in roads comprise only a tiny fraction of pixels they reside within, making their detection difficult. The incorporation of texture based measures in CART analysis in future research may improve results.

INTRODUCTION

It is estimated that each Californian pays an average of $558 every year in vehicle maintenance and repair costs due to driving on substandard roads. For the entire state, this totals $12 billion per year. While California is rated as having the worst roads in the country, the problem exists nationwide. The use of hyperspectral imagery may provide a cost-effective way to monitor the condition of roads on a regular basis, allowing prioritization of road improvements and rapid response to time sensitive conditions such as potholes. In June, 2004, hyperspectral imagery and high resolution aerial photographs were collected over Valencia in southern California for the purpose of road condition assessment. The hyperspectral data is from the HyperSpecTIR instrument, which collects data in 227 spectral bands spanning the VNIR and SWIR ranges, and in this case has a spatial resolution of 2 meters.

Objective

The objective of this study is to utilize hyperspectral data to accurately classify road conditions and identify potholes in a semi-automated manner. The high resolution aerial photography is used to assist in verifying road conditions and the location of potholes. The results of this study could be used to take another step towards the

* Current information: Systems Engineer, Santa Barbara Infrared, Inc., 30 South Calle Cesar Chavez, Suite D, Santa Barbara, CA 93103, jlaveigne@sbir.com

utilization of hyperspectral imagery by state and local governments to improve road conditions and reduce cost incurred by motorists.

DATA

Two types of data were used for this study. The first is hyperspectral imagery, used for the spectral detection of various road conditions. The second is high resolution aerial photography, used to supplement available ground truth photos for selecting training pixels. These training pixels are then used as the basis for mapping road quality in the hyperspectral imagery. Data from both instruments were collected simultaneously from the same aircraft on May 5, 2004 over Valencia, California. Valencia is approximately 40 miles northwest of downtown Los Angeles. Data collection focused on major thoroughfares in the area: Magic Mountain Parkway and San Fernando Road.

Hyperspectral Imagery

The HyperSpecTIR (HST) instrument used in this study is constructed and operated by SpecTIR Corporation. HST consists of two boresighted spectrometers collecting 227 contiguous, non-overlapping bands covering the reflective spectral range from 0.45-2.45um. Band spacings and widths vary from about 12 nanometers in the visible and near infrared (VNIR) spectrometer to 8 nanometers in the short-wave infrared (SWIR) spectrometer. The instrument has a 1 milliradian instantaneous field of view (IFOV), equating to 1 meter ground sampling distance (GSD) per kilometer above ground level (AGL). HST uses a two-dimensional focal plane, in which one dimension of 256 pixels is used for spatial data and the other dimension of 256 pixels is used for spectral data. Note that because of spectrometer overlap and pixels reserved for collecting bright and dark calibration data, the final dataset consists of 227 spectral bands. HST is operated as a line scanner, resulting in a swath that is 256 pixels wide by *n* pixels long, where *n* depends upon the scan width. The resulting flightline is therefore a series of "bricks," with a nominal amount of overlap between each brick. Differential GPS and inertial navigation system (INS) data are recorded to provide information for subsequent georeferencing. HST utilizes beam steering optics technology to control mirror motion in order to cancel out any distortions caused by the pitch, roll, and yaw of the platform. This technology allows HST to fly at low altitudes (normally very turbulent) in order to collect high spatial resolution data and ensure that there are no gaps in the data resulting from platform motion. To date, HST has collected imagery with spatial resolutions as high as 0.5 meters.

The flightline used for this study focused on San Fernando Road. This flightline spans approximately 4.8km with 21 swaths, each swath being 0.42km wide. One swath in this flightline has been corrupted, so was not included in the analysis. The data were converted to reflectance by SpecTIR using a proprietary MODTRAN based technique.

Aerial Photography

The aerial photography for this study was collected at the same time from the same platform (Cessna 206) as the hyperspectral imagery. The camera used is a medium format camera using a Zeiss 50mm lens mounted in a Leica gimbal ring mount. Ultraviolet and infrared restricting filters are used to generate a true color image. The camera is controlled by a TrackAir survey type flight management system, and data is collected on a Kodak K3 Blue Series chip (4000 x 4000 pixels), processed out to a 48 megabyte RGB file. For this study, the aircraft was flown at 2500 feet above ground level at 100 knots, producing 1 foot ground sampling distances. Frames were captured with 30% forward overlap at five second intervals.

METHODS

The methods described here were used to extract the road network from the hyperspectral imagery and to classify them by road condition. Unless otherwise noted, all methods are implemented within Research Systems' ENVI™ image processing software.

Rule Generator

The Rule Generator is a tool that utilizes classification and regression tree (CART) algorithms to generate a set of rules that, when applied to an image, result in a classified product. Rule Generator is an ENVI plug-in written by the author that makes use of the freeware CART algorithms Quick, Unbiased and Efficient Statistical Tree (QUEST) (Loh and Shih, 1997), and Classification Rule with Unbiased Interaction Selection and Estimation (CRUISE) (Kim and Loh, 2001). Interested parties may download Rule Generator for free from the RSI User-Contributed Library at http://www.rsinc.com/codebank/index.asp. QUEST and CRUISE may be downloaded separately from http://www.stat.wisc.edu/~loh/loh.html.

The classification and regression tree (CART) approach is an automated way of determining statistical relationships between a number of independent variables given a set of dependent data. This approach has been used for a number of years in many disciplines, and is now seeing increasing use in remote sensing. In the remote sensing case, the independent variables could include continuous data such as spectral bands, elevation, slope, vegetation indices, and so on. Independent variables may also include categorical data such as classifications. Dependent variables are the training data. A series of regression analyses are performed between the independent and dependent variables to create a set of rules. These rules are in the form of a decision tree, where each node is some condition such as "band x is less than or equal to y." The leaf nodes represent the final classes that the pixels will be assigned to.

The CART approach has been most commonly applied to multispectral classification, although hyperspectral applications have shown promise (Smith *et al*, 2004). When many independent variables are used (such as the many bands of a hyperspectral dataset), CART tends to select a subset of bands that provide the greatest ability to separate the input classes. This study uses this band subset to compare with other methods and to perform further classification.

As mentioned above, CART has the ability to incorporate ancillary data sets as independent variables. For road extraction purposes, available road vector databases available from the state or county could be used to more accurately extract roads while reducing confusion with roofs and parking lots. Since no ancillary data were available for this study, though, this approach was not undertaken.

BandMax

BandMax is an ENVI tool that produces a subset of spectral bands that optimizes the separability of a target spectrum from background spectra through the use of spectral contrast measures. Therefore, BandMax is used in this study to determine the optimal bands to distinguish road types from each other.

Spectral Angle Mapper

The Spectral Angle Mapper (SAM) algorithm is an automated method for comparing one spectrum to another. For example, the spectrum at each pixel in an image may be compared one at a time to some reference spectrum, such as a mineral in a spectral library. The SAM algorithm determines the similarity between two spectra by calculating the "spectral angle" between them, treating each spectrum as a vector in space with dimensionality equal to the number of bands (Kruse et al., 1993). One advantage of this technique is that it is relatively insensitive to illumination conditions, such as those resulting from topography and cross-track illumination. Because these illumination variations do not always occur equally to every band, it is not a complete solution.

Each pixel in the resultant SAM image is assigned a value representing its spectral angle relative to the reference spectrum. The smaller the value, the smaller the angle, and the closer the match between the target and reference spectra. Therefore, darker pixels on a SAM image indicate increasing similarity between the image spectrum and the reference spectrum. Because only the smallest angles are likely to actually be the target material, a threshold is used to provide an image with better contrast. That is, every pixel whose value exceeds a set threshold will be displayed as white instead of some varying shade of gray. This allows easy discrimination of pixels with good matches.

Supervised Minimum Distance Classification

The Minimum Distance classifier calculates the Euclidean distance between each pixel's spectrum and the mean spectrum for each training group. The class with the minimum distance is assigned to the pixel (Richards, 1999). Whereas the Spectral Angle Mapper classifier is relatively insensitive to the overall albedo difference between target and reference spectra, the Minimum Distance classifier is highly sensitive to this albedo difference. Results from these methods will provide a useful indicator for the importance of albedo in mapping road conditions.

Spectral Similarity Mapper

The Spectral Similarity Mapper (SSM) is a custom ENVI plug-in written in the IDL programming language by the author. It is derived from the Spectral Similarity Scale described by Sweet *et al* (2000). SSM calculates two numbers for each pixel. The first is the Euclidean distance between the pixel's spectrum and the reference spectrum. The second is a correlation value, which measures the similarity in shape between the pixel's spectrum and reference spectrum, much like SAM does. The Spectral Similarity Value (SSV) is derived from these two values by (Sweet *et al*, 2000):

$$SSV = \sqrt{d_e^2 + \hat{r}^2} \qquad \text{(EQ 1)}$$

where d_e represent the Euclidean distance measure and r represents the correlation measure.

Therefore, SSM is a hybrid approach combining elements of both the SAM and Minimum Distance classifier methods described above into a single measure.

VIS2 and SWIR Ratios

Previous work by Herold et al (2004) suggest that spectral ratios at different locations in the spectrum could map road condition. The VIS2 ratio (830nm/490nm) relates to the relative increasing brightness of worn asphalt, and the increasing spectral concavity of worn asphalt in this region due to iron oxide absorptions. The SWIR ratio (2120nm/2340nm) decreases with increasing road age and deterioration primarily due to reduced hydrocarbon absorption in this spectral region.

EXPERIMENT

The experiment involved creating a discrete classification of the roads within the hyperspectral imagery that would depict the varying level of surface conditions. A discrete classification rather than continuous "surface quality" layer was selected due to the lack of *a priori* knowledge of the spectral characteristics of a "good" road versus a "bad" road.

Pre-Processing

The first step in creating this classified product was devising a classification scheme. Because the spatial resolution of the hyperspectral data was not fine enough for the literal observation of potholes, cracking, and other road condition indicators, the aerial photography was used for a visual survey of the existing road conditions. In addition to the aerial photography, select locations within the study area were visited and photographed by an assistant (Figure 1). Together, the aerial and ground photography led to an initial breakout of the following classes: Road (excellent, medium, and worn), Cracked Road (light, medium, and severe), and Patch.

Figure 1 – Example of a ground photo used to assist in locating damaged roads in the aerial imagery.

Training points were then collected by a single individual through literal exploitation of the aerial and ground photography, then locating the corresponding position in the hyperspectral data. The data were not georeferenced for this study, so training points were transferred from the aerial photography to the hyperspectral image by relative positioning relative to common features such as parked cars, painted road lines, etc. Because both image sources were collected simultaneously, this method is quite accurate.

Because of the spatially discontinuous nature of damaged asphalt, training points were selected pixel by pixel, rather than as lines or regions. This limited the total number of training points selected. In addition, the imagery was collected with no *a priori* knowledge of road conditions, resulting in there being only limited areas of damaged road surface to train on. Once training point selection was completed, the mean spectrum of each category was compared with the other category mean spectra to determine its spectral separability. Because the classes being selected for this study are all very similar, some of the selected classes were determined not to be separable. Those classes determined not to be separable were combined. Finally, the training points were split into training and validation sub-groups by stratified random sampling. Figure 2 shows hyperspectral and aerial photograph chips for each class.

One of the objectives of this study is to determine whether any particular subset of spectral bands produces more accurate results than using all the spectral bands. Band subsets were selected in several ways. The first way was to feed QUEST and CRUISE the training points and have them determine the optimal subset of bands needed to classify the data. These algorithms go one step further and provide specific relationships between these bands to produce a classified image, but in this case we are only interested in which bands are selected. Another method to select a band subset was BandMax. BandMax produces a plot showing the significance values of each band for separating a target spectrum from a background spectrum or spectra. For this study, each training category was input as a target spectrum with the remaining classes comprising the background spectra. The resulting significance vectors were then summed in order to identify which bands were most significant in differentiating the targets from the background. Finally, a random subset of 20 bands was selected to test whether the "smart" ways of choosing band subsets were really all that smart.

Classification

The training points were then used as input to the classification methods described previously. The SAM, Minimum Distance, and SSM classifiers were each run successively using all spectral bands (minus those in atmospheric absorption bands), and spectral band subsets determined by QUEST, CRUISE, BandMax, and randomly. Classifications resulting from QUEST and CRUISE may only be produced by the band subset that they themselves select. Figures 3 and 4 show the band subsets used for BandMax, QUEST, and CRUISE. Figure 5 shows the spectral library generated by calculating the mean spectrum for each set of training pixels.

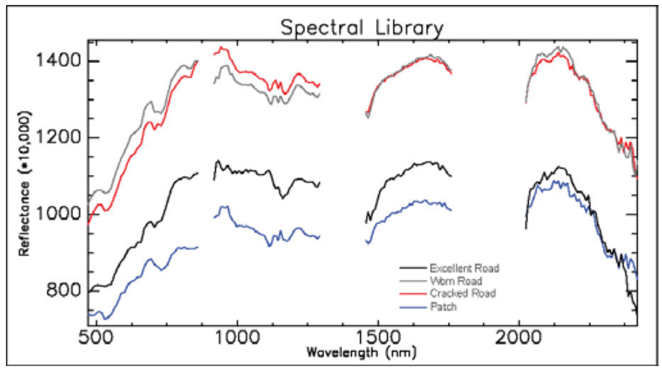

Figure 5 – Spectral library containing average spectrum for each class.

A road mask was used so that the resulting classification image only reflected results for roads, with every other pixel being set to *Unclassified*. The road mask was generated through a combination of spectral and spatial means. SAM was used to generate rule images for the Excellent Road and Worn Road classes. Road centerlines were then digitized manually on the hyperspectral imagery. ENVI's Decision Tree Classifier was then used to create a mask that passed those pixels that had a SAM value indicating a close match to either Excellent or Worn Road, and occurred within 8 pixels of a road centerline. Using the spatial measure was necessary to prevent the inclusion of parking lots and some roof types that are spectrally very similar to roads.

The accuracy of the classified products were then assessed by building confusion matrices that use the validation points. A comparison of classification results for the different methods are shown in Figure 6.

Comparison with VIS2 and SWIR Ratios

VIS2 and SWIR ratios were calculated as described in Herold *et al* (2004). These results are compared with the classification results derived here by performing a linear regression on the ratio values at each validation point location versus each validation pixels' class value. For VIS2, high values should correlate with our Cracked Road class. For SWIR, high values should correlate with our Excellent Road class.

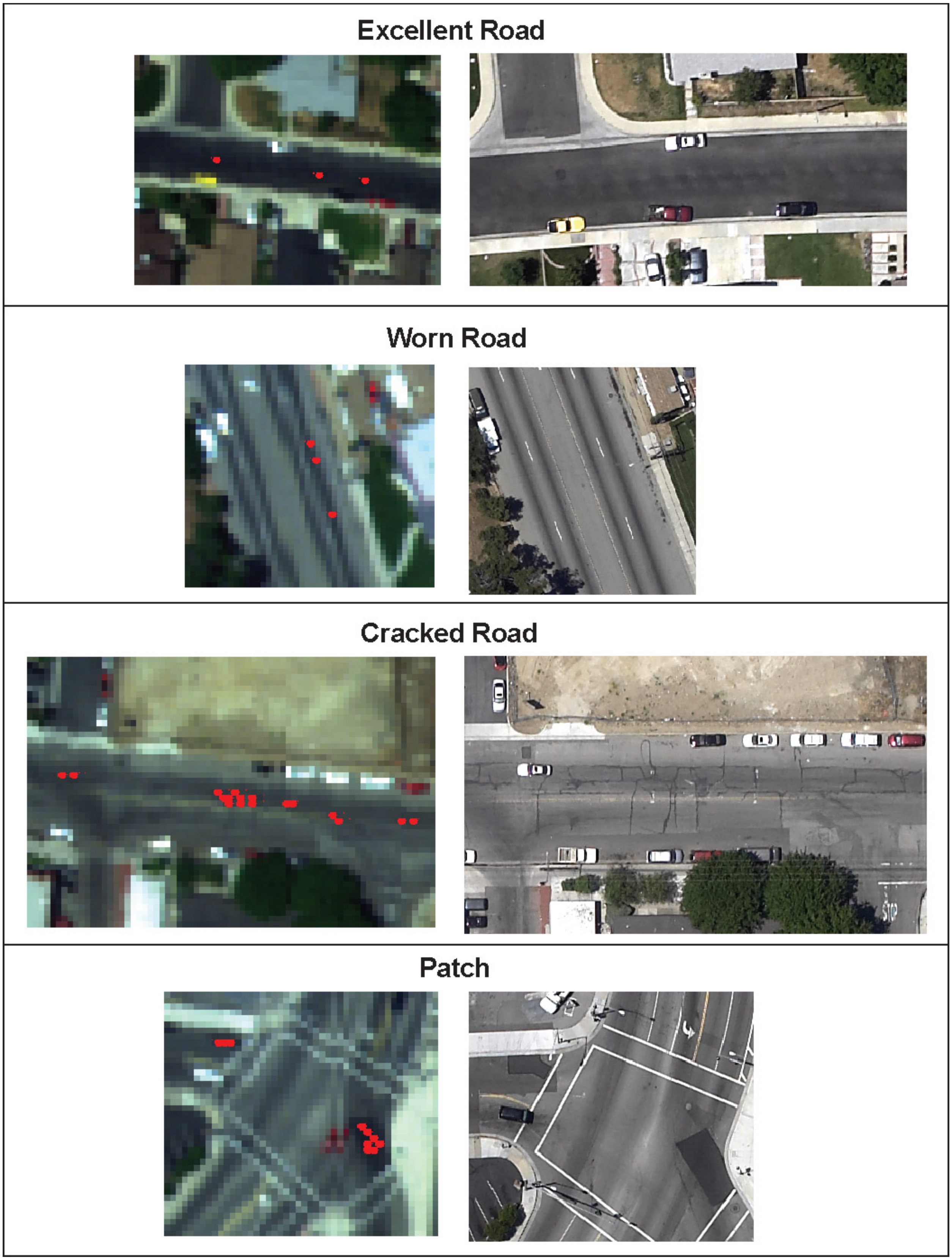

Figure 2 – Image chips from HyperSpecTIR (left) and aerial photography (right) showing representative samples of the classes that were trained on. Red pixels in the HST image chips represent a portion of the pixels used for training.

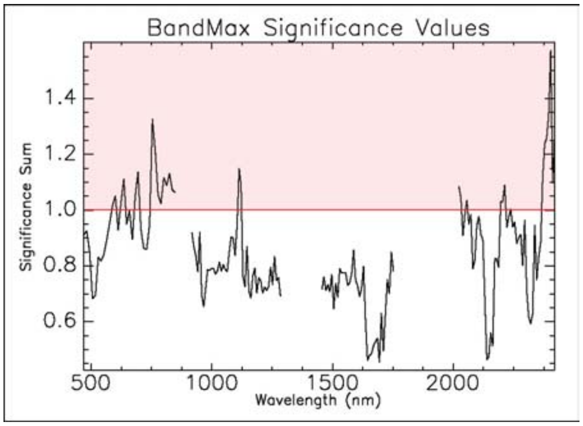

Figure 3 – Plot showing summed BandMax significance Values. Shaded area indicates bands that were selected For the BandMax spectral band subset.

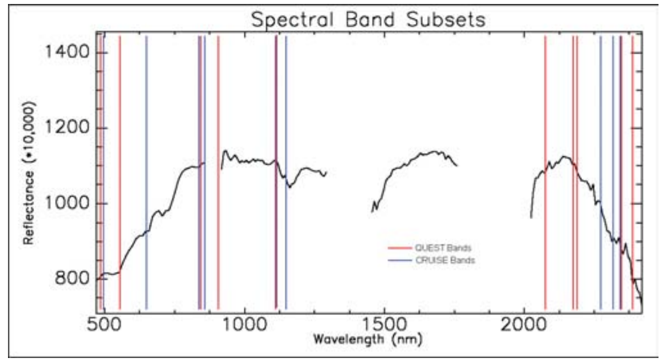

Figure 4 – Plot showing spectral band subsets as determined by QUEST and CRUISE.

RESULTS

The results of the accuracy assessment for the Minimum Distance classifier are shown in Table 1. Using all the spectral bands produced slightly more accurate results than other band subsets. All "smart" band subsets produced substantially more accurate results than the random band subset.

The results of the accuracy assessment for the Spectral Angle Mapper classifier are shown in Table 2. SAM produced the lowest overall accuracy of any classification method (~40%), with the best results being from the QUEST and CRUISE band subsets. All band subsets except for BandMax produced results better than a random subset.

The results of the accuracy assessment for the Spectral Similarity Mapper classifier are shown in Table 3. SSM produced accuracies similar to Minimum Distance, with the highest accuracy (54%) coming from all spectral bands. Interestingly, the accuracy resulting from a random selection of bands (50%) is nearly as good as using all bands, and is slightly better than results from all the "smart" band subset methods.

The results of the accuracy assessment for the QUEST and CRUISE algorithms are shown in Table 4. These CART-like methods produced the most accurate results of all the methods (61% and 68% respectively). Note that because of the nature of these algorithms, they could only be run on the spectral band subset that they select as part of the processing.

Figure 7 shows results for the VIS2 and SWIR ratio compared to a false color composite image. Figures 8 shows the linear regression performed between the VIS2 ratio and classification values. Figure 9 shows the same for the SWIR ratio. The correlation in each case is poor, suggesting no solid relationship. However, the trend of the fitted line to the SWIR ratio data does have the expected trend of lower SWIR ratio values for decreasing road condition. No trend is evident in the VIS2 ratio data.

DISCUSSION

Examination of the confusion matrices and accuracy assessments demonstrates the challenge of accurately mapping road surface conditions. The best results by a significant margin were those produced by the CART algorithm CRUISE. Following CRUISE came QUEST, then Minimum Distance and SSM (tied), and finally SAM. This ranking clearly indicates that albedo and not just spectral shape is a key indicator to road surface conditions.

The best performing classifiers (QUEST and CRUISE) used only about 15% of the available spectral bands (not including bands in atmospheric absorption regions). These bands were spread across the entire spectral region, indicating that there is no single key region that is particularly well suited for road quality mapping. However, when the band subsets that QUEST and CRUISE used were then used in the other classifiers, the results were not nearly as accurate, and were generally lower than when all bands were used in these classifiers. Because the produced decision trees from QUEST and CRUISE use specific data values as thresholds, the robustness of the technique is limited. Data from other areas would have to be atmospherically corrected, and the quality of the radiometric calibration becomes crucial.

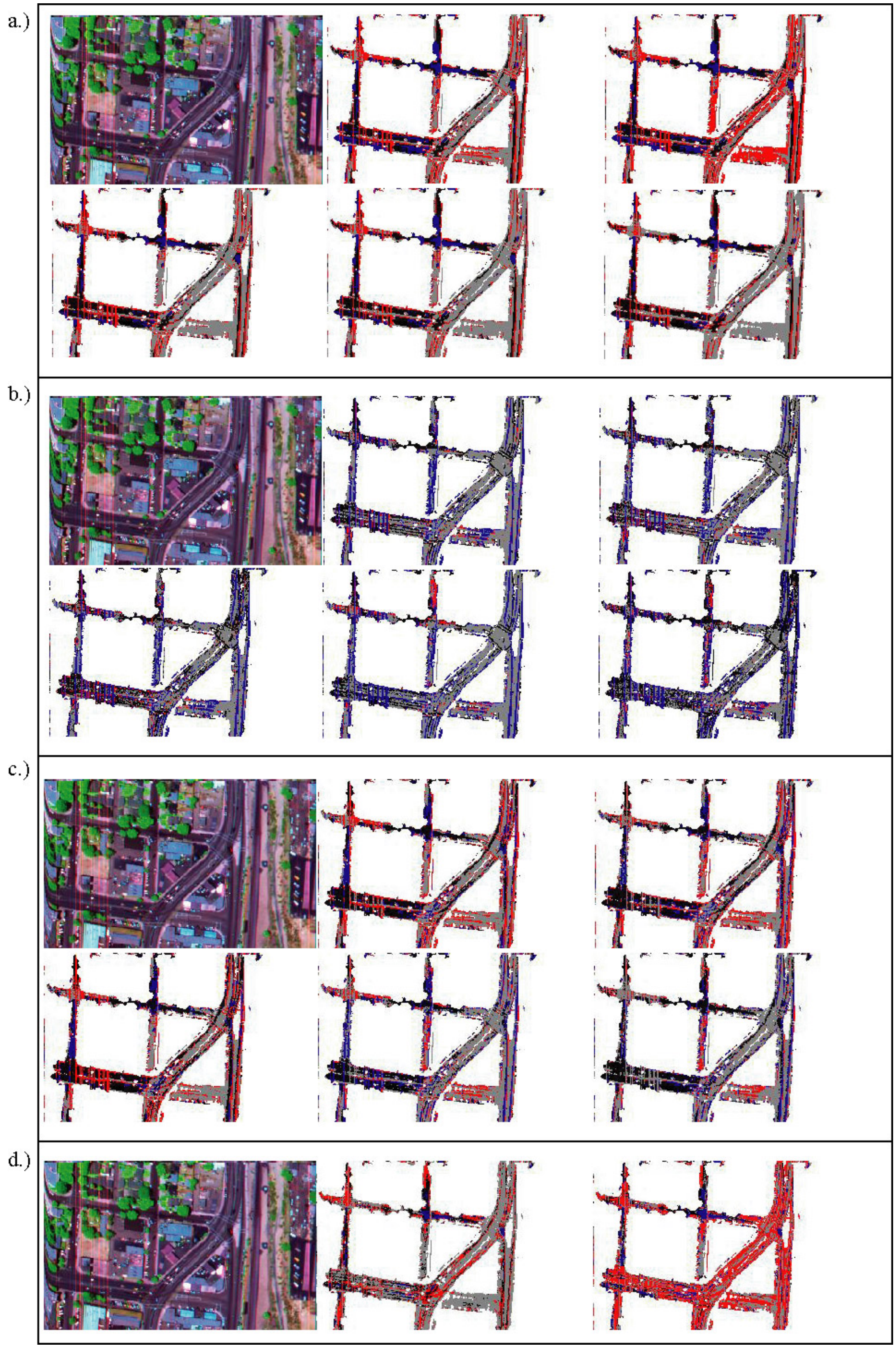

Figure 6 – Images showing classification results for the different methods used. First row, left to right: false color composite, all bands, random bands. Second row, left to right: QUEST bands, CRUISE bands, random bands. a.) Minimum Distance, b.) Spectral Angle Mapper, c.) Spectral Similarity Mapper, d.) CART algorithms (center: QUEST, right: CRUISE).

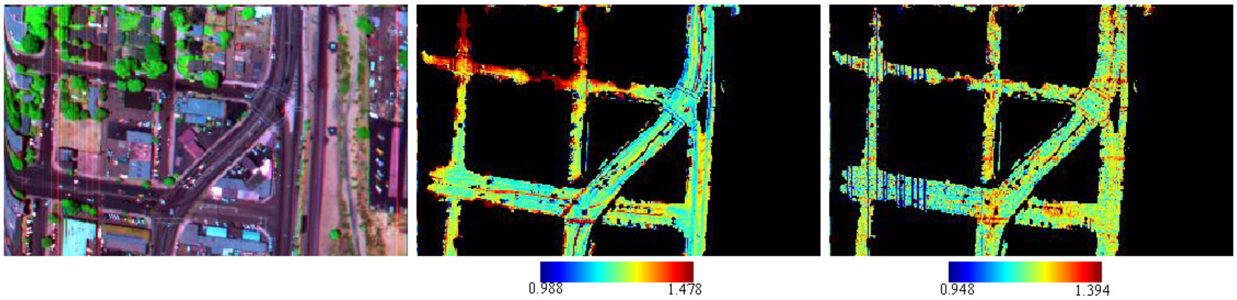

Figure 7 – Images showing ratio results for a portion of the study area (left: false color composite, center: VIS2 ratio, right: SWIR ratio). Observe that diffuse shadowing in the upper left portion of the VIS2 ratio makes the road appear to be more damaged than it actually is.

Table 1 – Accuracy assessment for the Minimum Distance classifier.

Minimum Distance

All Bands

Class	Patch	Excellent Road	Cracked Road	Worn Road	Total	Producer's Accuracy
Patch	8	5	0	2	15	100.00%
Excellent Road	0	0	2	4	6	0.00%
Cracked Road	0	5	19	6	30	82.61%
Worn Road	0	0	2	4	6	25.00%
Total	8	10	23	16	57	
User's Accuracy	53.33%	0.00%	63.33%	67.67%		**54.39%**

BandMax Bands

Class	Patch	Excellent Road	Cracked Road	Worn Road	Total	Producer's Accuracy
Patch	5	5	0	1	11	62.50%
Excellent Road	3	1	1	5	10	10.00%
Cracked Road	0	4	17	4	25	73.91%
Worn Road	0	0	5	6	11	37.50%
Total	8	10	23	16	57	
User's Accuracy	45.45%	10.00%	68.00%	54.55%		**50.88%**

QUEST Bands

Class	Patch	Excellent Road	Cracked Road	Worn Road	Total	Producer's Accuracy
Patch	5	5	0	1	11	62.50%
Excellent Road	3	0	2	5	10	0.00%
Cracked Road	0	5	17	5	27	73.91%
Worn Road	0	0	4	5	9	31.25%
Total	8	10	23	16	57	
User's Accuracy	45.45%	0.00%	62.96%	55.56%		**47.37%**

CRUISE Bands

Class	Patch	Excellent Road	Cracked Road	Worn Road	Total	Producer's Accuracy
Patch	8	5	0	2	15	100.00%
Excellent Road	0	0	2	4	6	0.00%
Cracked Road	0	5	17	5	27	73.91%
Worn Road	0	0	4	5	9	31.25%
Total	8	10	23	16	57	
User's Accuracy	53.33%	0.00%	62.96%	55.56%		**52.63%**

Random Bands

Class	Patch	Excellent Road	Cracked Road	Worn Road	Total	Producer's Accuracy
Patch	8	5	0	2	15	100.00%
Excellent Road	0	0	2	4	6	0.00%
Cracked Road	0	4	12	8	24	52.17%
Worn Road	0	1	9	2	12	12.50%
Total	8	10	23	16	57	
User's Accuracy	53.33%	0.00%	50.00%	16.67%		**38.60%**

Table 2 – Accuracy assessment for the Spectral Angle Mapper classifier.

Spectral Angle Mapper

All Bands

Class	Patch	Excellent Road	Cracked Road	Worn Road	Total	Producer's Accuracy
Patch	1	1	2	4	8	12.50%
Excellent Road	0	6	10	5	21	60.00%
Cracked Road	1	2	9	1	13	39.13%
Worn Road	6	1	2	6	15	37.50%
Total	8	10	23	16	57	
User's Accuracy	12.50%	28.57%	69.23%	40.00%		38.60%

BandMax Bands

Class	Patch	Excellent Road	Cracked Road	Worn Road	Total	Producer's Accuracy
Patch	1	1	5	6	13	12.50%
Excellent Road	1	6	12	5	24	60.00%
Cracked Road	1	1	5	1	8	21.74%
Worn Road	5	2	1	4	12	25.00%
Total	8	10	23	16	57	
User's Accuracy	7.69%	25.00%	62.50%	33.33%		28.07%

QUEST Bands

Class	Patch	Excellent Road	Cracked Road	Worn Road	Total	Producer's Accuracy
Patch	2	1	2	4	9	25.00%
Excellent Road	0	7	7	6	20	70.00%
Cracked Road	0	1	12	4	17	52.17%
Worn Road	6	1	2	2	11	12.50%
Total	8	10	23	16	57	
User's Accuracy	22.22%	35.00%	70.59%	18.18%		40.35%

CRUISE Bands

Class	Patch	Excellent Road	Cracked Road	Worn Road	Total	Producer's Accuracy
Patch	1	1	5	5	12	12.50%
Excellent Road	0	8	7	5	20	80.00%
Cracked Road	0	0	9	1	10	39.13%
Worn Road	7	1	2	5	15	31.25%
Total	8	10	23	16	57	
User's Accuracy	8.33%	40.00%	90.00%	33.33%		40.35%

Random Bands

Class	Patch	Excellent Road	Cracked Road	Worn Road	Total	Producer's Accuracy
Patch	1	1	3	4	9	12.50%
Excellent Road	0	6	8	6	20	60.00%
Cracked Road	1	3	10	5	19	43.48%
Worn Road	6	0	2	1	9	6.25%
Total	8	10	23	16	57	
User's Accuracy	11.11%	30.00%	52.63%	11.11%		31.58%

Table 3 – Accuracy assessment for the Spectral Similarity Mapper classifier.

Spectral Similarity Mapper

All Bands

Class	Patch	Excellent Road	Cracked Road	Worn Road	Total	Producer's Accuracy
Patch	4	0	1	1	6	50.00%
Excellent Road	4	5	0	4	13	50.00%
Cracked Road	0	5	18	7	30	78.26%
Worn Road	0	0	4	4	8	25.00%
Total	8	10	23	16	57	
User's Accuracy	66.67%	38.46%	60.00%	50.00%		54.39%

BandMax Bands

Class	Patch	Excellent Road	Cracked Road	Worn Road	Total	Producer's Accuracy
Patch	2	1	3	4	10	25.00%
Excellent Road	5	6	1	4	16	60.00%
Cracked Road	0	3	12	2	17	52.17%
Worn Road	1	0	7	6	14	37.50%
Total	8	10	23	16	57	
User's Accuracy	20.00%	37.50%	70.59%	42.86%		45.61%

QUEST Bands

Class	Patch	Excellent Road	Cracked Road	Worn Road	Total	Producer's Accuracy
Patch	4	0	1	1	6	50.00%
Excellent Road	4	5	0	4	13	50.00%
Cracked Road	0	1	16	9	26	69.57%
Worn Road	0	4	6	2	12	12.50%
Total	8	10	23	16	57	
User's Accuracy	66.67%	38.46%	61.54%	16.67%		47.37%

CRUISE Bands

Class	Patch	Excellent Road	Cracked Road	Worn Road	Total	Producer's Accuracy
Patch	1	1	4	3	9	12.50%
Excellent Road	5	6	1	5	17	60.00%
Cracked Road	0	3	13	4	20	56.52%
Worn Road	2	0	5	4	11	25.00%
Total	8	10	23	16	57	
User's Accuracy	11.11%	35.29%	65.00%	36.36%		42.11%

Random Bands

Class	Patch	Excellent Road	Cracked Road	Worn Road	Total	Producer's Accuracy
Patch	3	1	1	1	6	37.50%
Excellent Road	5	5	0	5	15	50.00%
Cracked Road	0	3	19	8	30	82.61%
Worn Road	0	1	3	2	6	12.50%
Total	8	10	23	16	57	
User's Accuracy	50.00%	33.33%	63.33%	33.33%		50.88%

Table 4 – Accuracy assessment for the the CART classifiers.

QUEST

Class	Patch	Excellent Road	Cracked Road	Worn Road	Total	Producer's Accuracy
Patch	6	1	0	1	8	75.00%
Excellent Road	2	5	1	5	13	50.00%
Cracked Road	0	3	16	2	21	69.57%
Worn Road	0	1	6	8	15	50.00%
Total	8	10	23	16	57	
User's Accuracy	75.00%	38.46%	76.19%	53.33%		61.40%

CRUISE

Class	Patch	Excellent Road	Cracked Road	Worn Road	Total	Producer's Accuracy
Patch	8	2	0	3	13	100.00%
Excellent Road	0	7	1	2	10	70.00%
Cracked Road	0	1	19	6	26	82.61%
Worn Road	0	0	3	5	8	31.25%
Total	8	10	23	16	57	
User's Accuracy	61.54%	70.00%	73.08%	62.50%		68.42%

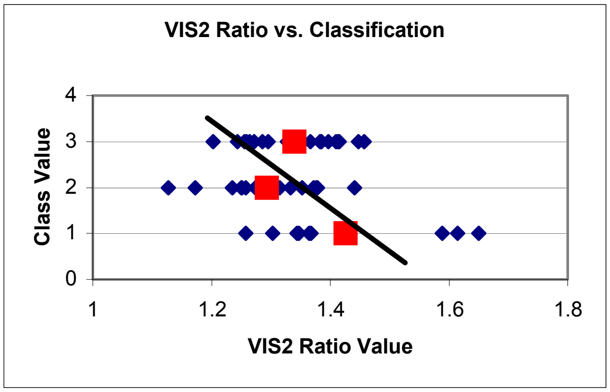

Figure 8 – Chart showing correlation between VIS2 ratio and classified results.

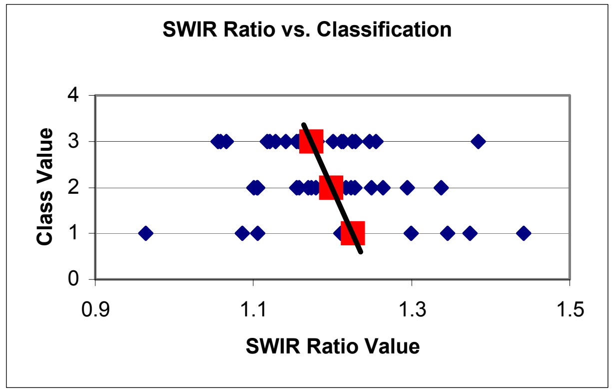

Figure 9 – Chart showing correlation between SWIR ratio and classified results.

In terms of robustness, the Minimum Distance and Spectral Similarity Mapper routines perform equally well, even though their accuracies are not much better than 50%. Because these methods do not use threshold values, they are less sensitive to calibration issues.

The relatively low classification accuracies are not very surprising, considering the nature of the features being mapped. Like vegetation, another notoriously difficult material to map, all of our classes are comprised of the same basic components. In this case, it's asphalt. While properties of asphalt may vary regionally depending on the mixtures and types of components (tar, gravel, sand, etc.), the asphalt within our study area is not likely to vary much. The spectral library (Figure 5) shows that Worn Road and Cracked Road are extremely similar. This is logical, considering that cracks are likely to occur more often in worn roads than fresh roads. The faces of the cracks themselves and the material filling them (if any), which together comprise a tiny fraction of an HST pixel, are solely responsible for any spectral differentiation. As can be seen in the classified images (Figure 6), it is evident that the abundance of Cracked Road is overestimated while Worn Road is underestimated. Considering the subtle spectral differentiation between these classes, especially since the cracks may be filled or not filled, a better approach may be to incorporate a texture layer to observe the more mottled nature of cracked pavement. Higher spatial resolution in the hyperspectral imagery would also improve results, even though this would lessen the value of hyperspectral imagery relative to aerial photography.

There was essentially little to no correlation between these classified products and road quality measures found in the literature. The VIS2 and SWIR ratio products also were not very successful in identifying damaged roads, though, and seem to be highly affected by any shadowing. Even diffuse shadowing severely affected the ratio results, making these areas appear to be more highly damaged than they actually were.

CONCLUSIONS

This study had only modest success at mapping road quality with hyperspectral imagery. This success is tempered by the fact that detailed training needed to be performed using high spatial resolution aerial photography. Considering the extremely variable nature of these road classes, it is unlikely that the derived spectral library could be applied to a different area with much success.

One solid conclusion, though, is that any method used to map road quality with spectral data must include some measure of albedo in addition to spectral shape. The CART-like algorithms used here proved to be superior to other methods, though their robustness is limited. The addition of a texture measure (easily included in CART analysis along with spectral data) may improve results.

ACKNOWLEDGEMENTS

The authors would like to thank SpecTIR Corporation and IK Curtis Services for graciously providing their data at no cost for this study. Much thanks also go to Jennifer Jengo and Steven Kugies for their willingness to give up a weekend day to go take pictures of asphalt.

REFERENCES

Herold, M, Roberts, D., Smadi, O, and Noronha, V. (2004). Road Condition Mapping with Hyperspectral Remote Sensing. *Proceedings of the 2004 AVIRIS Workshop*. Pasadena, CA-USA.

Jensen, J.R. (1996). *Introductory Digital Image Processing: A Remote Sensing Perspective*. Prentice Hall, Upper Saddle River, NJ, pp.229-231.

Kim, H. and Loh, W.-Y. (2001). Classification trees with unbiased multiway splits. *Journal of the American Statistical Association*, 96:589-604.

Kruse, F.A., Lefkoff, A.B., Boardman, J.W., Heidebrecht, K.B., Shapiro, A.T., Barloon, P.J., and Goetz, A.F.H. (1993). The Spectral Image Processing System (SIPS) – Interactive Visualization and Analysis of Imaging Spectrometer Data. *Remote Sensing of Environment*, 44:145-163.

Loh, W.-Y. and Shih, Y.-S. (1997). Split selection methods for classification trees. *Statistica Sinica*, 7:815-840.

Richards, J.A. (1999). *Remote Sensing Digital Image Analysis*. Springer-Verlag, Berlin, p. 240.

Smith, F.G.F., Jengo, C. (2004). The Classification of Hyperspectral Data Using the CART Classification Approach. *Proceedings of the ASPRS 2004 Annual Meeting*. Denver, CO-USA.